XRD and FTIR Characterisation of Lead Oxide-Based Pigments and Glazes

Jurate Senvaitiene, Junona Smirnova, Aldona Beganskiene, Aivaras Kareiva*

Department of General and Inorganic Chemistry, Vilnius University, Naugarduko 24, LT-03225 Vilnius, Lithuania.
Tel.: +370 5 2193110, Fax: +370 5 2330987, E-mail: aivaras.kareiva @chf.vu.lt.

Abstract

This article covers the results of application of X-ray powder diffraction (XRD) and Fourier transform infrared spectroscopy (FTIR) in assessing the chemical and phase composition of ancient pigments, glazes and glazed pottery samples. In order to demonstrate the reliability of above mentioned techniques, the XRD and FTIR analyses were performed on the representative samples of the lead oxide (Pb_3O_4 or $PbCO_3 \times Pb(OH)_2$) based pigments and glazes. The analyzed glaze compositions contained silica and calcite as main constituents and pigments lead-tin yellow, smalt, Verona green, manganese black, Naples yellow and malachite as secondary phases. XRD analysis and FTIR spectroscopy have proven to be useful tools for qualitative determination of the composition of glazes. However, in some cases many problems concerning the identification of separate phases are still to be solved using other analytical techniques.

Keywords: pigments, glazes, pottery, XRD, FTIR, cultural heritage

1. Introduction

Conservation scientists in the field of glass, ceramics, paper, metals and alloys, work on preserving an item without disturbing the structure of the raw material.[1–8] The preparation of low cost and environmentally benign technological procedures for the conservation of ancient pottery still is a problem. Ceramics are composite in nature and are prepared from different starting materials, with certain technologies. The final product consists of many different phases including crystalline and glassy ones, along with unreacted starting materials. The composition of the ceramic body and of the applied glaze, where present, is critically dependent on the processing technologies, firing sequence and the kiln temperatures.[9–11] The conservation process can be greatly influenced by specific chemical reactions appearing due to the different chemical compositions in the object of conservation and protective coatings.[9,12,13] Thus, to avoid the possible interactions careful characterization of ceramic sample should be done.[14–17]

Moreover, the physical-chemical characterization of pottery used in ancient times could provide historical and technological information as regards their manufacture and to solve specific historical problems.[18–20] The knowledge of chemical and mineralogical compositions is mandatory in characterization studies of pottery: the former

mainly depends on the raw materials used to produce the wares but also on processing and depositional changes, the latter on both the initial composition and the processing, as minerals are the "fingerprints" of the stable and also the metastable solid phases formed during firing.[21,22]

It is well known that the characterization of glazed pottery is very specific and complicated since the glaze is usually composed of many different pigments.[23,24] Consequently these ceramic samples have a rather complex chemistry.[25–27] In the present study, attention has been focused on the characterization of lead oxide based pigments and glazes using X-ray diffraction analysis and FTIR spectroscopy. The lead oxides along with different additives were widely used as pigments and glazes mostly for the decoration of pottery since antiquity.[28–31] Moreover, these pigments are highly variable in texture, lustre and hardness. The identification of pigments in their mixtures or on unknown ceramic samples is very important not only for the characterization of materials, but also for nondestructive conservation and successful restoration, dating and authentication.[22,32,33]

2. Experimental

Analytical grade reagents (Kremer Pigmente) were used for the preparation of lead oxides based glazes. The samples analyzed are described in Table 1.

Table 1. List and chemical compositions of the glazes analysed.

Sample No	Composition* (molar ratio)
1	$Pb_3O_4 : SiO_2$ = 3.625 : 0.875
2	$Pb_3O_4 : SiO_2 : CaCO_3$: lead-tin yellow = 3.625 : 0.875 : 0.25 : 0.25
3	$Pb_3O_4 : SiO_2 : CaCO_3$: smalt = 3.625 : 0.875 : 0.25 : 0.25
4	$Pb_3O_4 : SiO_2 : CaCO_3$: Verona green = 3.625 : 0.875 : 0.25 : 0.25
5	$Pb_3O_4 : SiO_2 : CaCO_3$: manganese black = 3.625 : 0.875 : 0.25 : 0.25
6	$Pb_3O_4 : SiO_2 : CaCO_3$: Naples yellow = 3.625 : 0.875 : 0.25 : 0.25
7	$Pb_3O_4 : SiO_2 : CaCO_3$: malachite = 3.625 : 0.875 : 0.25 : 0.25
8	Lead white : $SiO_2 : CaCO_3$: Naples yellow = 3.625 : 0.875 : 0.25 : 0.25
9	Lead white : SiO_2 : Naples yellow = 3.625 : 0.875 : 0.25

* Lead-tin yellow – $SnO \times SiO_2 \times PbO$; smalt – $K_2O \times SiO_2 \times Co_3O_4$;
Verona green – $K(Mg,Fe)(Fe,Al)Si_4O_{10}(OH)_2$; manganese black – MnO_2;
Naples yellow – $Sb_2O_5 \times 2PbO$; malachite – $Cu(OH)_2 \times CuCO_3$; lead white – $PbCO_3 \times Pb(OH)_2$.

The individual pigments, their mixtures and the glazes obtained by high temperature firing of starting materials at 1000 °C were used for analytical characterization. In some cases the glazed pottery samples were investigated as well.

The prepared samples were characterized by non-destructive analytical techniques. The X-ray powder (XRD) analysis was performed with a Siemens D-500 diffractometer equipped with a conventional X-ray tube (Cu-$K\alpha_1$ radiation (λ = 1.54060 Å), power conditions (40 kV/30 mA)). The germanium monochromated X-rays have been collected using linear PSD (opening angle: $2\theta = 6°$). The XRD patterns were measured in the range of 20 to 70° 2θ with the step size of 0.02° and 30 s counting per step at room temperature (25 °C). For infrared (FTIR) studies, a Perkin-Elmer FT-IR Spectrum BX II apparatus was used. The samples were mixed (1.5%) with dried KBr and pressed into pellets.

3. Results and Discussion

3.1. X-ray Diffraction Analysis

The X-ray diffraction pattern of the mixture of lead oxide and quartz (sample 1) is shown in Figure 1. As seen in the XRD pattern of sample 1, the both oxides (Pb_3O_4 and SiO_2) could be easily identified, and no other peaks attributable to unknown phases were detected.

The next step was to use the XRD technique for the qualitative determination of secondary phases in the similar glazes having more complicated chemical compositions. As seen from Table 1, most of the glazes contain $CaCO_3$ in their compositions. Additionally, the mixtures 2, 3, 4 and 5 contain different pigments such as lead-tin yellow, smalt, Verona green and manganese black. For comparison, the XRD patterns of individual pigments were also recorded. The XRD patterns of $CaCO_3$, lead-tin yellow, smalt, Verona green and manganese black are shown in Figures 2–5.
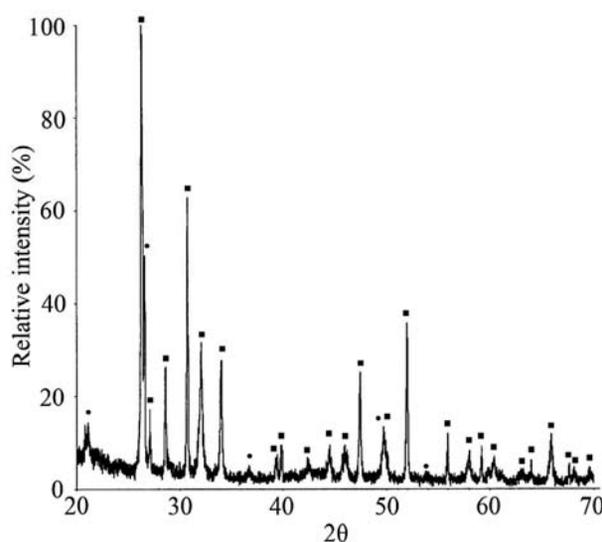

Figure 1. XRD pattern of the mixture of Pb_3O_4 (■) : SiO_2 (●) = 3.625 : 0.875.
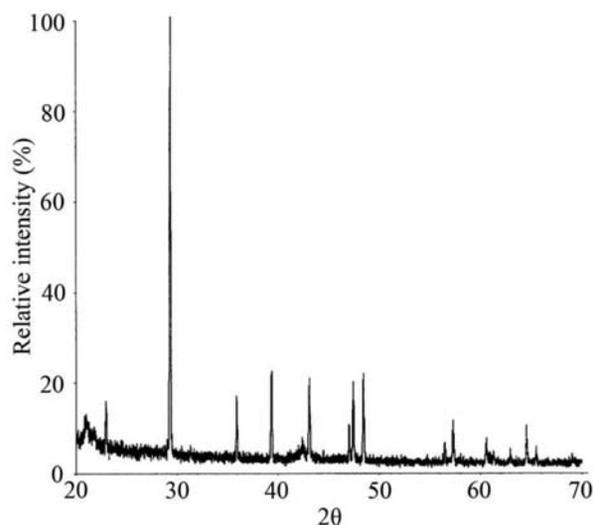

Figure 2. XRD pattern of $CaCO_3$.

Figure 2 shows only diffraction lines attributable to $CaCO_3$ phase (PDF 72-1937). In the XRD spectrum of lead-tin yellow pigments (see Figure 3) the diffraction lines from quartz and $SnO \times PbO$ pigment (PDF 17-607) could be easily identified. On the other hand, the XRD patterns of smalt and Verona green (Figure 4a and b, respectively) are amorphous. The low crystallinity may be detected and for manganese black pigment (Figure 5), however, this is in a good agreement with reference data (PDF 24-735). Figure 6 shows the XRD patterns of glazes 2–5 from Table 1.
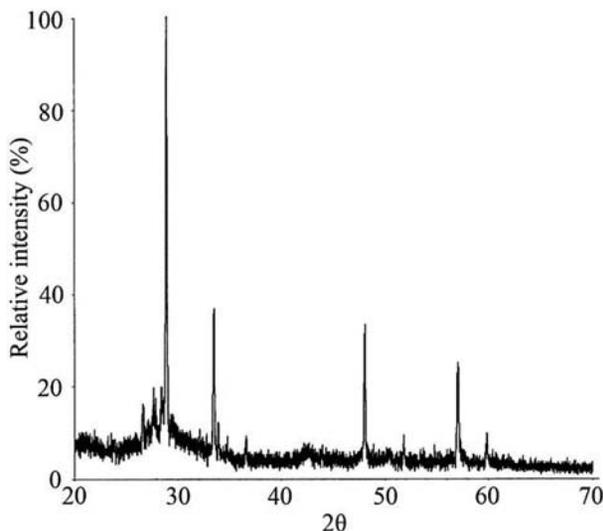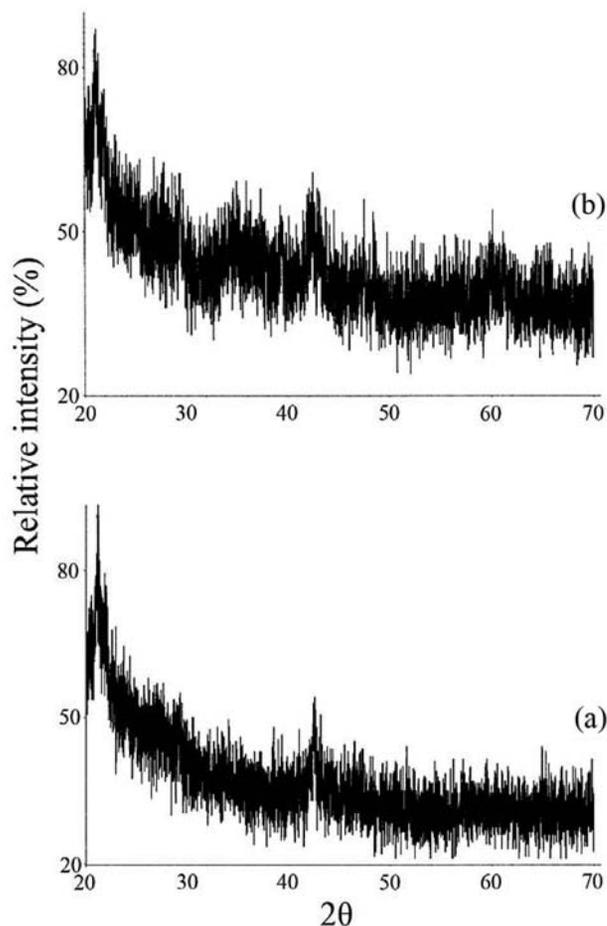

Figure 3. XRD pattern of lead-tin yellow.

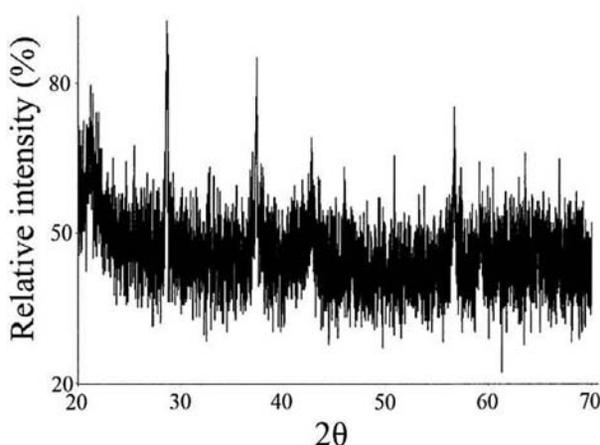**Figure 4.** XRD patterns of smalt (a) and Verona green (b).

Figure 5. XRD pattern of manganese black.

As seen, the main peak of $CaCO_3$ at around 2θ = 29.5° clearly persists in all XRD patterns presented in Figure 6. However, the lead-tin yellow pigment is hardly to detect in Figure 6a. It is evident from Figures 2 and 3 that the positions of main peaks of $CaCO_3$ and lead-tin yellow are located almost at the same 2θ value. Therefore, these

diffraction lines may be overlapped in the XRD pattern of glaze 2. Apparently, the amorphous phases, smalt and Verona green, are not detectable by XRD analysis (Figures 6b and c, respectively). On the other hand the small amount of manganese black in the composition of lead oxide based glazes could be identified by XRD analysis (see Figure 6d). The X-ray diffraction patterns of two second representative samples (glazes 6 and 7) are shown in Figure 7.

Evidently, the XRD pattern displayed in Figure 7a and shows the presence of Naples yellow and in Figure 7b – malachite. The XRD pattern of Naples yellow is shown in Figure 8.

The X-ray diffraction peaks around $2\theta \approx 30$ and 49.5° represent the most intensive diffraction lines of $Sb_2O_5 \times 2PbO$ (PDF 74-1354). These peaks are present in Figure 7a as well. Figure 9 shows the XRD pattern of malachite.

According to JCPDS© reference data, Figure 9 represents typical X-ray diffraction spectrum of $Cu(OH)_2 \times CuCO_3$ (PDF 76-660). The most intensive lines of XRD pattern of malachite observed at 2θ between 24 and 30° are also present in Figure 7b. Finally, the X-ray diffraction patterns of two last investigated samples (glazes 8 and 9) are shown in Fig 10.
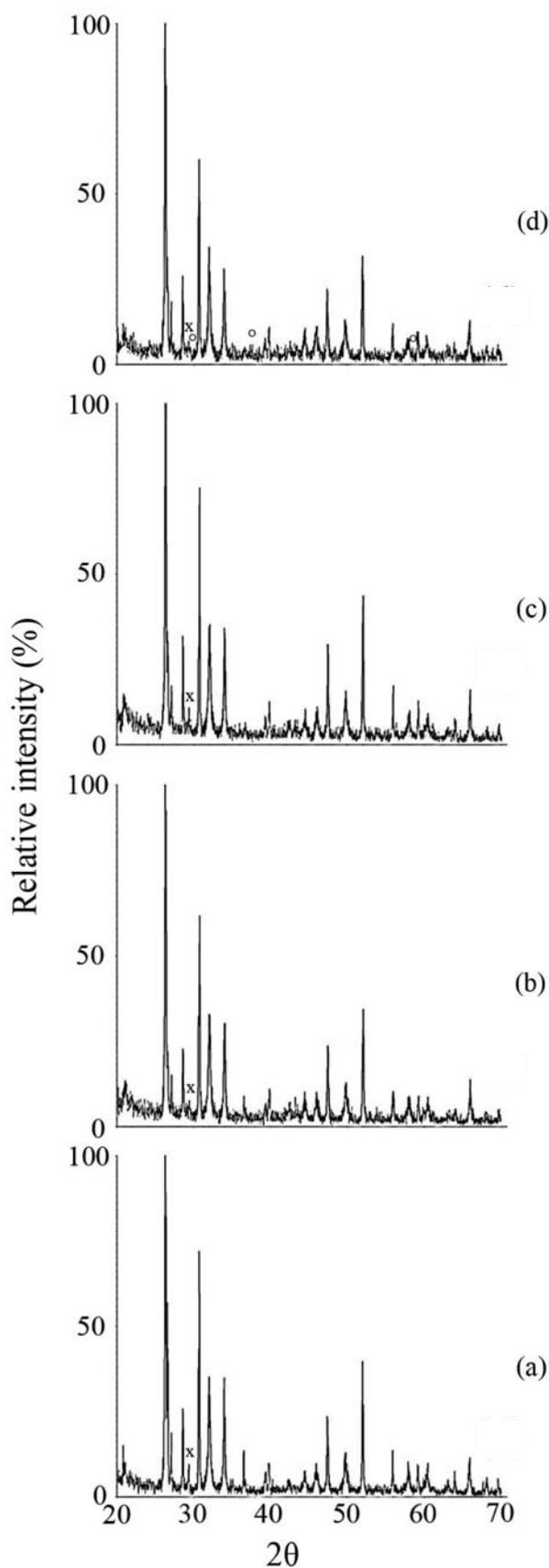
Figure 6. XRD patterns of different samples: sample 2 (a), sample 3 (b), sample 4 (c) and sample 5 (d). The secondary phases are marked: $CaCO_3$ (x) and MnO_2 (□).
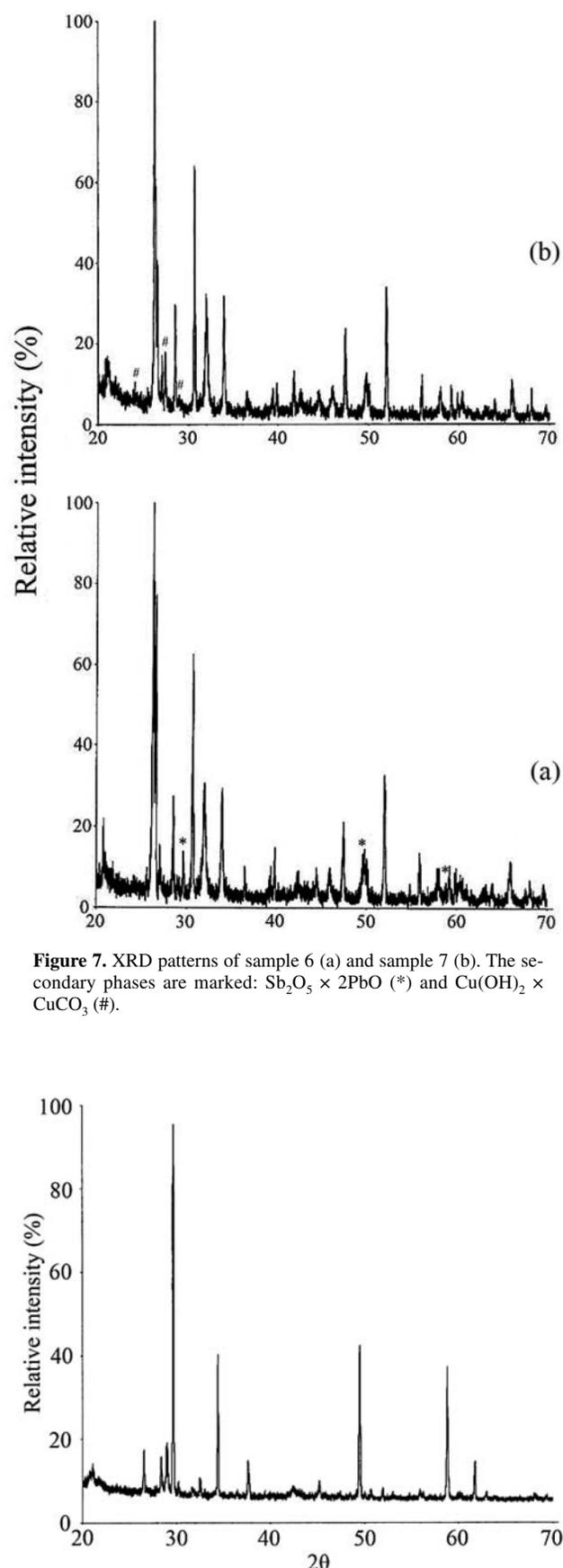

Figure 7. XRD patterns of sample 6 (a) and sample 7 (b). The secondary phases are marked: $Sb_2O_5 \times 2PbO$ (*) and $Cu(OH)_2 \times CuCO_3$ (#).
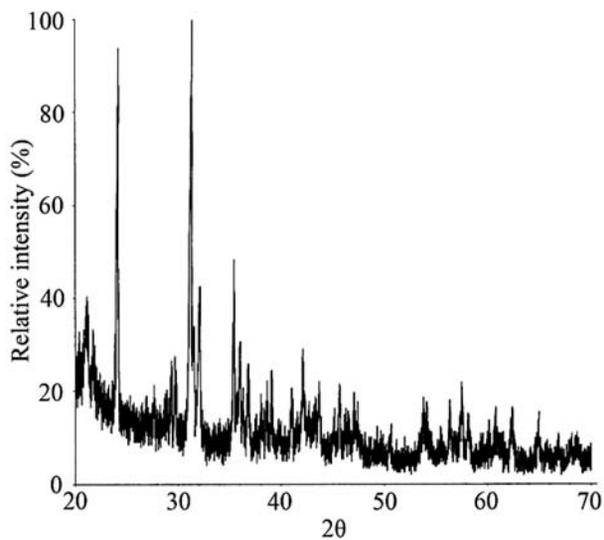

Figure 8. XRD pattern of Naples yellow.

Figure 9. XRD pattern of malachite.

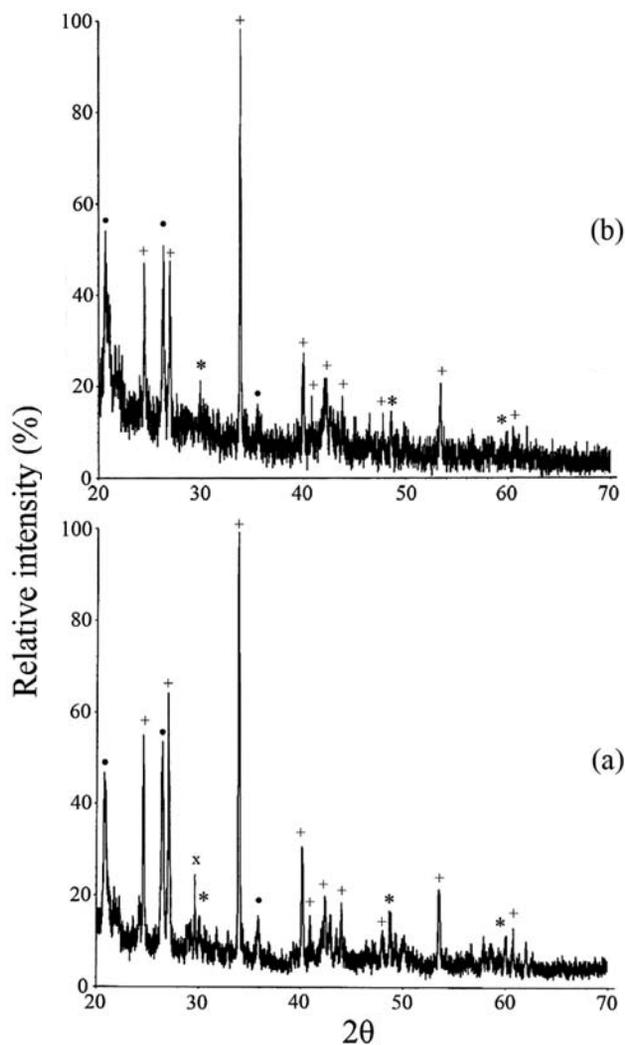**Figure 10.** XRD patterns of sample 8 (a) and sample 9 (b). The main and secondary phases are marked: $PbCO_3 \times Pb(OH)_2$ (+), Si-O_2 (●), $Sb_2O_5 \times 2PbO$ (*), and $CaCO_3$ (x).
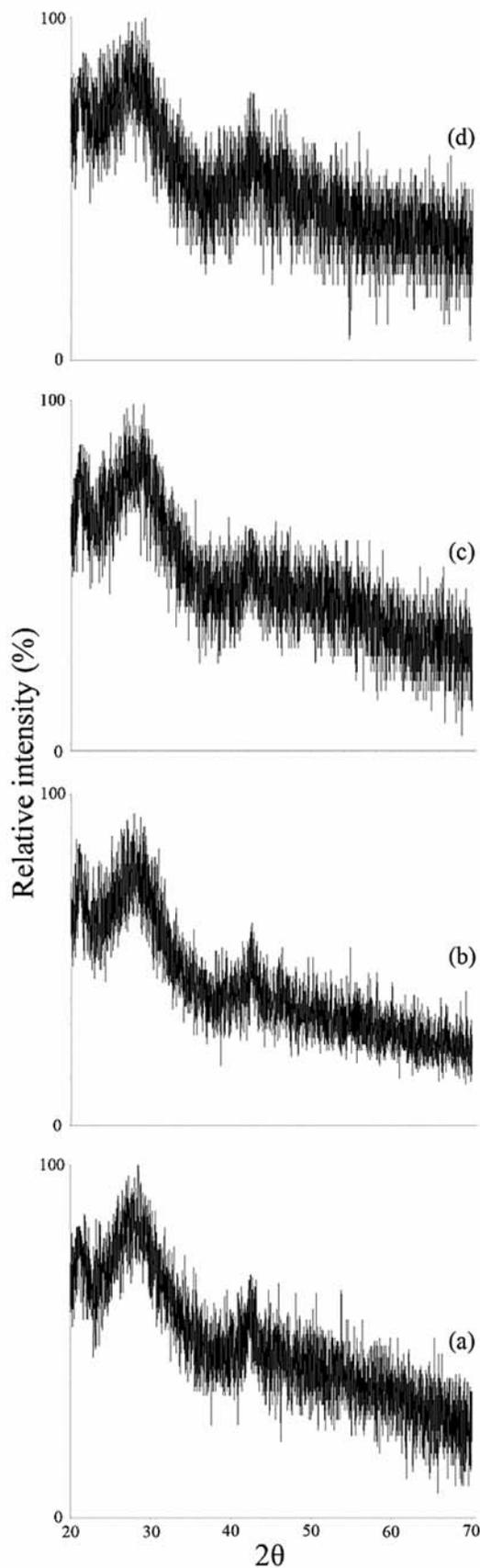

Figure 11. XRD patterns of fired at 1000 °C different glazes: sample 2 (a), sample 3 (b), sample 4 (c), and sample 6 (d).

The reflections from the main crystalline phase (Pb-$CO_3 \times Pb(OH)_2$) is dominating in the both XRD patterns, however, the secondary phases (silica and Naples yellow) may be also easily detected. The presence of the diffraction line at around $2\theta = 29.5°$ in the XRD spectrum of sample 8 (see Figure 10a) confirms once again that even small amounts of $CaCO_3$ in the mixtures of lead oxide based pigments could be determined by XRD analysis.

The glazes listed in Table 1 were calcined at 1000 °C, and again analyzed using X-ray diffraction technique. However, all fired samples were found to be amorphous to X-ray. The XRD patterns of the representative glazes are shown in Figure 11.

Therefore, the characterization of calcined lead oxide based glazes by XRD technique seems to be complicated indicating that other methods of analysis should be applied. The glazed pottery samples were also checked. Figure 12 shows the XRD patterns of the pottery specimens glazed with samples 5 and 7.
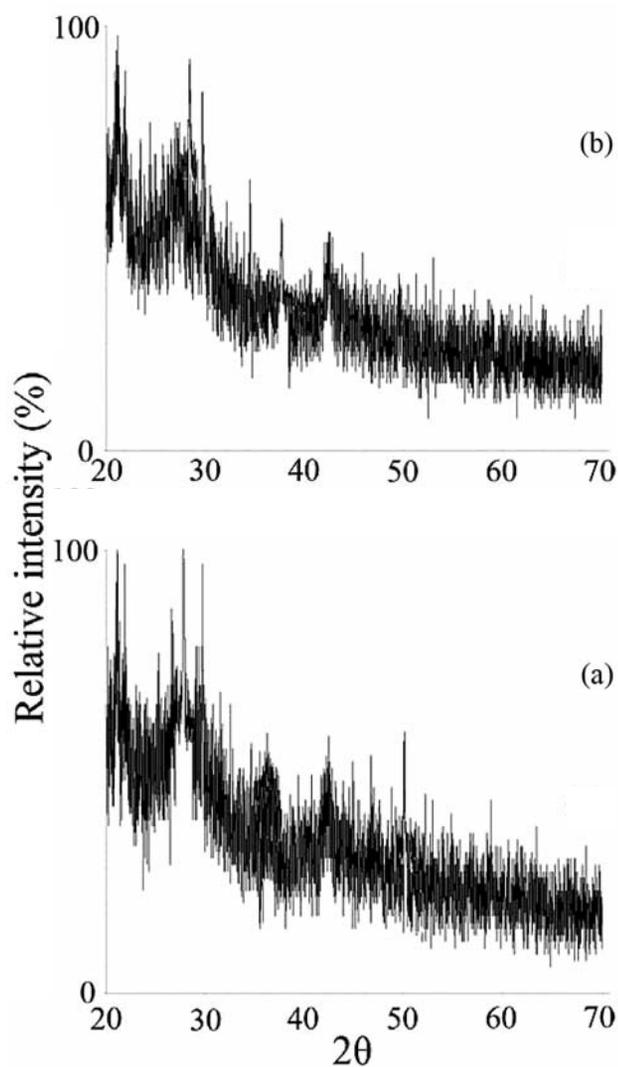

Figure 12. XRD patterns of glazed pottery with sample 5 (a) and sample 7 (b).

As seen, the XRD patterns of both samples are almost identical. The main part of XRD patterns confirms the amorphous character of the investigated samples. However, few diffraction lines are also visible. The most intensive peaks presented in the XRD patterns at around $2\theta = 26 – 28°$ indicate the presence of big amount of pottery itself (Figure 13).
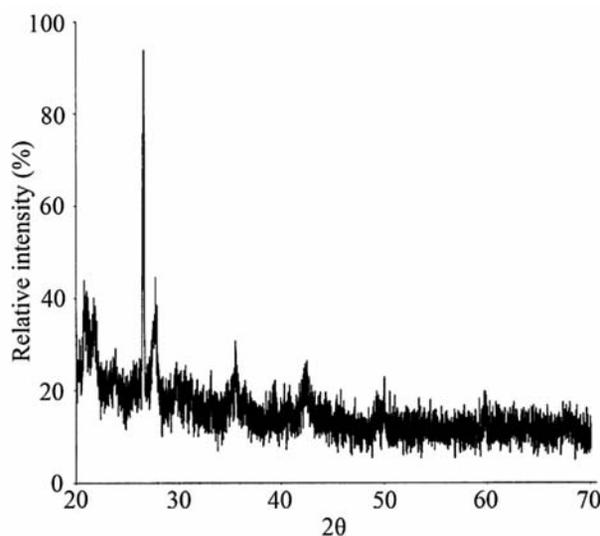

Figure 13. XRD pattern of pottery calcined at 1000 °C.

From these data it is possible to state that the XRD analysis results could be useful to distinguish glazed and non-glazed pottery samples.

3.2. FTIR Spectroscopic Analysis

It is well known, that definite substances can be identified by their FTIR spectra, interpreted like fingerprints.[34–36] To facilitate the interpretation of the XRD results the glazes and glazed pottery samples were also analyzed by FTIR spectroscopy. Figure 14 shows FTIR spectra for the glaze samples 1 and 2.

The absorptions from the main quartz phase (Si–O) could be also easily identified in the FTIR spectrum of mixture of lead oxide and silica (Figure 14a; 1163, 1083, 798, 778, 695, 514 cm^{-1}).[14] The several intense bands in the range 800–550 cm^{-1} (725, 646, 584 cm^{-1}) are characteristic of the metal-oxygen vibrations (possibly Pb–O) in the ceramic samples.[37, 38] Figure 14b shows FTIR spectrum of the glaze sample 2 which additionally contains calcite and lead-tin yellow. The similar bands attributable to the typical Si–O in quartz (1163, 1083, 798, 778, 695, 514 cm^{-1}) vibrations are very well resolved in the FTIR spectrum of glaze 2. However, additionally the characteristic carbonate (calcite phase) vibrations at 1795, 1430, 876, 713 cm^{-1},[35, 39] and M–O vibrations at 725, 685, 642, 580, 531 cm^{-1} could be also determined. We can only pre-
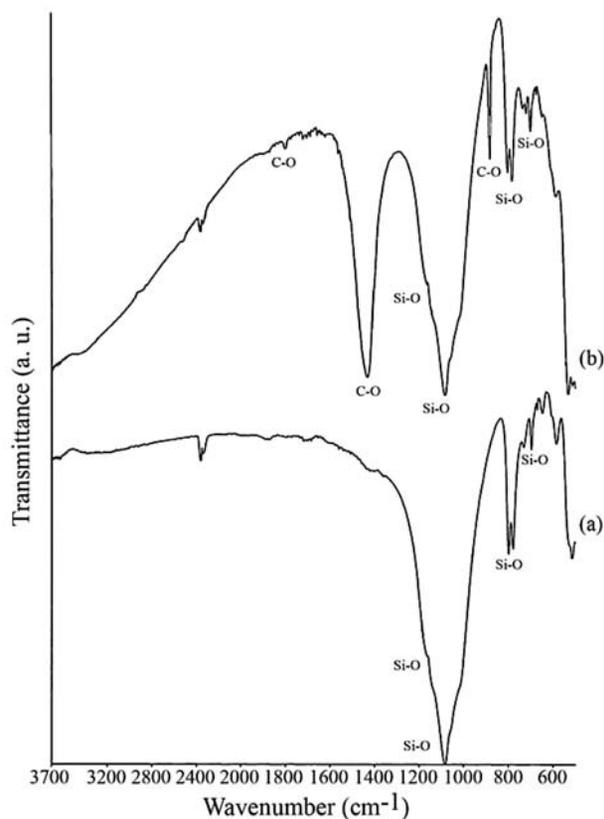
Figure 14. FTIR spectra of sample 1 (a) and sample 2 (b).

dict that observed additional peaks in Figure 14b at 685 and 531 cm^{-1} could be attributed to the Sn–O vibrations.

All FTIR spectra for the samples 2–9, however, were very similar regardless of the chemical composition. The FTIR spectra of three representative glaze samples are presented in Figure 15.

As seen, characteristics Si–O, C–O and M–O stretchings could be easily identified in all FTIR spectra. Moreover, broad bands between 3700–3000 cm^{-1} can be assigned to the adsorbed water (or water of crystallization) and O–H vibrations.[35,39] Thus, from the FTIR measurements only few components of lead oxide based glazes could be determined. For the identification of specific features of secondary phases such as lead-tin yellow, smalt, Verona green, manganese black, Naples yellow, malachite, or lead white the Raman or far infrared spectroscopies could be more effectively employed.[40–42]

Interestingly, the FTIR spectroscopy could be successfully applied for the identification of just obtained and fired at elevated temperatures glaze specimens. The FTIR spectra of glaze 8 before and after calcination at 1000 °C presented in Figure 16a and b, respectively, illustrate this observation. FTIR spectrum of glaze 8 presented in Figure 16a shows almost identical characteristics vibrations as those supplied in Figure 15. However after firing of the sample at 1000 °C some specific changes in the FTIR spectrum of glaze 8 (see Figure 16b) are evident. The cha-
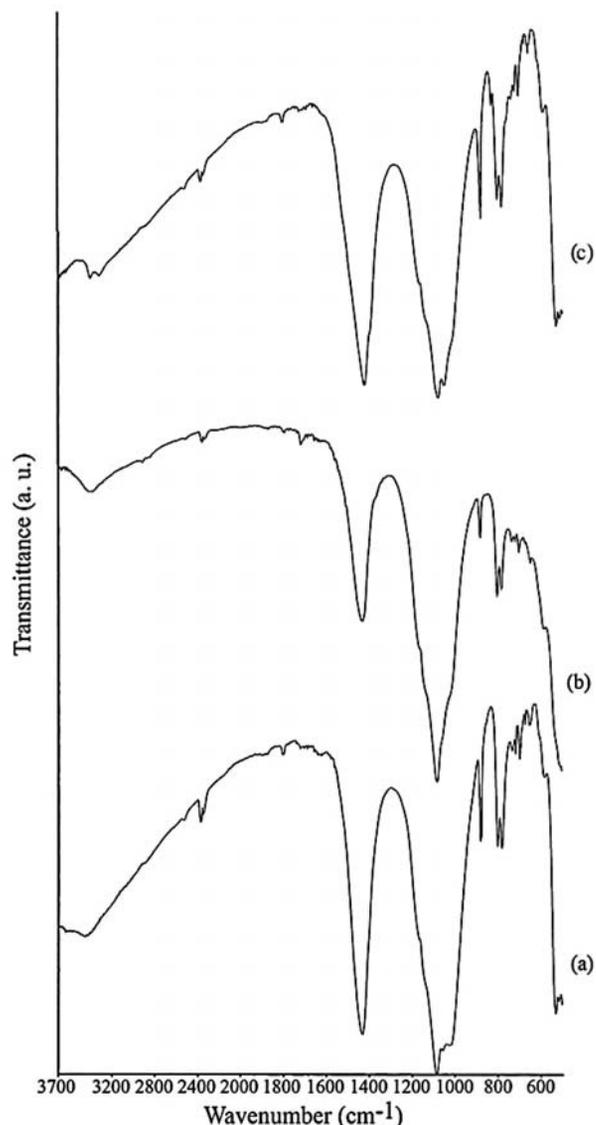

Figure 15. FTIR spectra of sample 3 (a), sample 4 (b) and sample 7 (c).

racteristic carbonate vibrations at 1794, 1430, 876, 712 cm^{-1} and O–H vibrations at 3700–3000 cm^{-1} are absent in the FTIR spectrum of the sample obtained after calcinations. These results indicate that full decarbonation and dehydratation of glaze occurs during high-temperature firing.

The FTIR spectra for glazed pottery samples were also checked. Figure 17 shows the FTIR spectra of the fired glaze 5 and pottery specimen glazed with the same glaze.

Again, FTIR spectra for glaze and glazed pottery specimens were almost identical. The carbonate peaks are not visible anymore in the FTIR spectra of calcined products. However, the broad band between 3700–3000 cm^{-1} assigned to the O–H vibrations is seen in the FTIR spectrum of glazed pottery. This could be associated
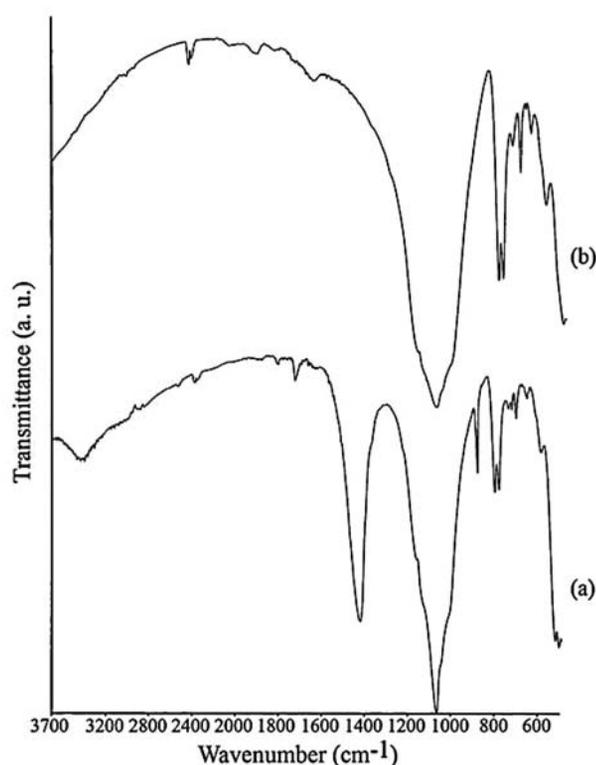
Figure 16. FTIR spectra of sample 8: just obtained (a) and fired at 1000 °C (b).
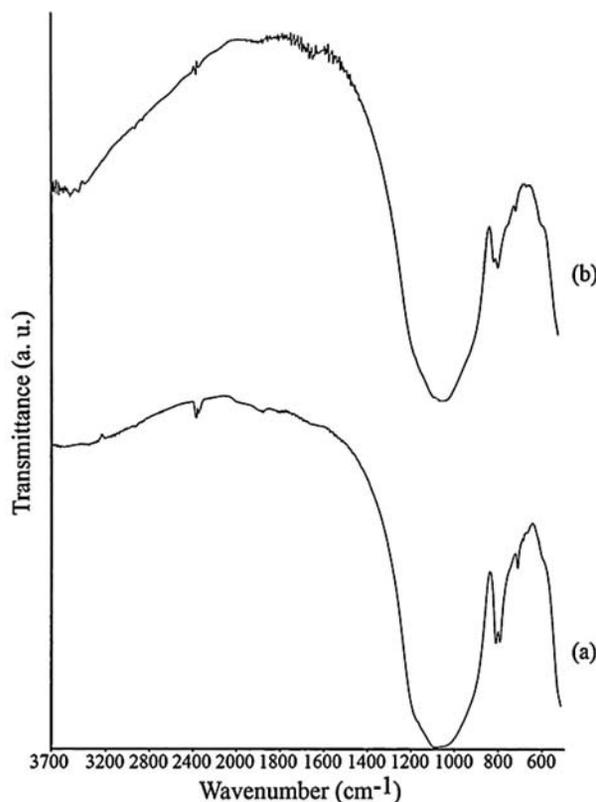

Figure 17. FTIR spectra of fired at 1000 °C sample 5 (a) and glazed pottery with sample 5 (b)

with specific surface properties of pottery which stimulate adsorption of moisture from atmosphere at ambient conditions.

4. Conclusions

Lead oxide based pigments and glazes having different chemical composition were characterized by XRD analysis and FTIR spectroscopy. XRD analyses clearly showed that most of investigated specimens are polycrystalline materials composed by different phases which could be successfully determined by XRD analysis. However, the characterization of fired lead oxide based glazes by XRD technique seems to be complicated due to amorphous character of obtained samples. Moreover, we have demonstrated that FTIR spectroscopy is significant analytical tool for the characterization of ancient pigments, glazes and glazed pottery. The characteristics Si–O, C–O and M–O stretchings could be easily identified in the FTIR spectra of lead oxide based glazes. Moreover, the FTIR spectroscopy could be successfully applied for the identification of fired glazes and glazed pottery specimens. In conclusion, the results summarized in this paper are very important for the development of new methods for the conservation of glazed pottery.

6. References

1. S. Fairbrass, *Int. J. Adhes. Adhesiv.* **1995,** *15,* 115–120.
2. M. Guglielmi, *J. Sol-Gel Sci. Technol.* **1997,** *8,* 443–449.
3. J. D. Mackenzie, E. P. Bescher, *J. Sol-Gel Sci. Technol.* **2000,** *19,* 23–29.
4. E. P. Bescher, F. Pique, F. Stulik, J. D. Mackenzie, *J. Sol-Gel Sci. Technol.* **2000,** *19,* 215–218.
5. R. A. Caruso, M. Antonietti, *Chem. Mater.* **2001,** *13,* 3272–3282.
6. T. P. Chou, C. Chandrasekaran, S. Limmer, C. Nguyen, G. Z. Cao, *J. Mater. Sci. Lett.* **2002,** *21,* 251–255.
7. J., M., *Restaurator* **2004,** *25,* 94–103.
8. J. Kiuberis, S. Tautkus, R. Kazlauskas, I. Pakutinskiene, A. Kareiva. *J. Cult. Herit.* **2005,** *6,* 245–251.
9. G. Biscontin, M. Pellizon Birelli, E. Zendri, *J. Cult. Herit.* **2002,** *3,* 31–37.
10. P. Colomban, N. Q. Liem, G. Sagon, H. X. Tinh, T. B. Hoanh, *J. Cult. Herit.* **2003,** *4,* 187–197.
11. H. G. M. Edwards, P. Colomban, B. Bowden, *J. Raman Spectrosc.* **2004,** *35,* 656–661.

12. L. Armelao, A. Bassan, R. Bertoncello, G. Biscontin, S. Daolio, A. Glisenti, *J. Cult. Herit.* **2000**, *1*, 375–384.

13. J. Senvaitiene, I. Pakutinskiene, A. Beganskiene, S. Tautkus, R. Kazlauskas, A. Kareiva. *Polish J. Chem.* **2005**, *79*, 1575–1583.

14. G. E. De Benedetto, R. Laviano, L. Sabbatini, P. G. Zambonin, *J. Cult. Herit.* **2002**, *3*, 177–186.

15. A. E. Lavat, E. J. Baran, *Vibr. Spectr.* **2003**, *32*, 167–174.

16. N. V. Vagenas, C. G. Kontoyannis, *Vibr. Spectr.* **2003**, *32*, 261–264.

17. W. Hausler, *Hyperfine Interact.* **2004**, *154*, 121–141.

18. A. Bakolas, G. Biscontin, V. Contardi, E. Franceschi, A. Moropoulou, D. Palazzi, E. Zendri, *Thermochim. Acta* **1995**, *269/270*, 817–828.

19. G. Eramo, R. Laviano, I. M. Muntoni, G. Volpe, *J. Cult. Herit.* **2004**, *5*, 157–165.

20. P. Cardiano, S. Ioppolo, C. De Stefano, A. Pettignano, S. Sergi, P. Piraino, *Anal. Chim. Acta* **2004**, *519*, 103–111.

21. P. M. Rice, *Pottery Analysis – A Sourcebook*, University of Chicago Press, Chicago, **1987**.

22. M. A. Legodi, D. de Waal, Cryst. Eng. **2003**, *6*, 287–299.

23. D. A. Scott, L. S. Dodd, J. Furihata, S. Tanimoto, J. Keeney, M. R. Schilling, E. Cowan, *Stud. Conserv.* **2004**, *49*, 177–192.

24. C. Ricci, I. Borgia, B. G. Brunetti, A. Sgamellotti, B. Fabbri, M. C. Burla, G. Polidori, *Archaeometry* **2005**, *47*, 557–570.

25. M. O. Figueiredo, J. P. Veiga, T. P. Silva, J. P. Mirao, S. Pascarelli, *Nucl. Instr. Methods Phys. Res.* **2005**, *238*, 134–137.

26. C. Fortina, A. S. Barbone, I. T. Memmi, *Archaeometry* **2005**, *47*, 535–555.

27. G. Bolelli, V. Cannillo, L. Lusvarghi, T. Manfredini, C. Siligardi, C. Bartuli, A. Loreto, T. Valente, *J. Eur. Ceram. Soc.* **2005**, *25*, 1835–1853.

28. I. Rajta, M. A. Ontalba, E. Koltay, A. Z. Kiss, *Nucl. Instr. Methods Phys. Res.* **1997**, *130*, 315–319.

29. G. D. Smith, L. Burgio, S. Firth, R. J. H. Clark, *Anal. Chim. Acta* **2001**, *440*, 185–188.

30. S. Murfitt, *Rezepte für Keramikglasuren,* Verlag Haupt, Bern, Stuttgart, Wien, 2003.

31. G. E. De Benedetto, P. Acquafredda, M. Masieri, G. Quarta, L. Sabbatini, P. G. Zambonin, M. Tite, M. Walton, *Archaeometry* **2004**, *46*, 615–624.

32. L. Burgio, R. J. H. Clark, S. Firth, *Analyst* **2001**, *126*, 222–227.

33. G. D. Smith, R. J. H. Clark, *J. Cult. Herit.* **2002**, *3*, 101–105.

34. C. J. Brinker, G. W. Scherrer, *Sol-gel science: the physics and chemistry of sol-gel processing,* Academic Press, New York, **1990**.

35. B. Schrader, *Infrared and Raman spectroscopy: methods and applications,* VCH, Weinheim, **1995**.

36. A. Baranauskas, D. Jasaitis, A. Kareiva, *Vibr. Spectrosc.* **2002**, *28*, 263–275.

37. G. Westin, M. Nygren, *J. Mater. Sci.* **1992**, *27*, 1617–1625.

38. A. Leleckaite, A. Kareiva, H. Bettentrup, T. Jüstel, H.-J. Meyer, *Z. Anorg. Allg. Chem.* **2005**, *631*, 2987–2993.

39. K. Nakamoto, *Infrared and Raman spectra of inorganic and coordination compounds*, John Wiley and Sons, New York, **1986**.

40. P. Colomban, *Appl. Phys. A: Mater. Sci. Process.* **2004**, *79*, 167–170.

41. O. M. Hemeda, *J. Magn. Magn. Mater.* **2004**, *281*, 36–41.

42. L. G. Hwa, Y. R. Chang, W. C. Chao, *Mater. Chem. Phys.* **2004**, *85*, 158–162.

Povzetek

V prispevku je opisana uporaba rentgenske praškovne difrakcije in FT infrardeče spektroskopije pri določanju kemijske in fazne sestave pigmentov, glazur in keramike. Preiskovali smo pigmente in glazure pripravljene na osnovi svinčevih spojin Pb_3O_4 ali $PbCO_3 \cdot Pb(OH)_2$). Vzorci so vsebovali še silicijev dioksid in kalcit kot glavni komponenti in kot dodatke pigmente svinec-kositer rumeno, kobaltovo steklo, veronsko zeleno, manganov dioksid, neapeljsko rumeno in malahit. Metodi sta uporabni za kvalitativno določitev sestave, nekateri vzorci pa bi za identifikacijo vseh prisotnih faz zahtevali uporabo dodatnih analiznih metod.